Unconventional Resources 4 (2024) 100098

Contents lists available at ScienceDirect

Unconventional Resources

journal homepage: www.keaipublishing.com/en/journals/unconventional-resources/

Geochemical characterization and paleo-burial history modelling of unconventional resources: A case study from the Kimmeridge Clay Formation (KCF) in the UK North Sea

Akinniyi A. Akinwumiju *, Dorothy Satterfield

School of Built and Natural Environment, College of Science and Engineering, University of Derby, DE22 1GB, UK

ARTICLE INFO

Keywords:
Kimmeridge Clay Formation
UK North Sea
Unconventional resources
Geochemical characterization
1D basin modelling
Thermal maturity
Transformation ratio
Oil saturation

ABSTRACT

For several decades the UK North Sea has been a prolific oil and gas province, with numerous conventional oil and gas discoveries sourced predominantly by the Upper Jurassic to Lower Cretaceous Kimmeridge Clay Formation (KCF). In this study, we have combined the analysis of total organic carbon/pyrolysis and vitrinite reflectance geochemical data from KCF samples with 1D basin modelling to investigate the potential for shale oil and gas plays in the Outer Moray Firth region. The results of geochemical evaluation show that most of the samples have very good to excellent hydrocarbon generation potential and contain predominantly oil-prone Type-II kerogen. A few samples show a significant oil saturation index above 100 mgHC/gTOC, which indicate a good potential for producible shale oil. The modelling results suggest that vitrinite reflectance values for the KCF vary mainly between 0.51 and 1.15%R_o, with kerogen transformation of up to 86 %. This is indicative of early-oil to late-oil/early-gas maturity window at present day, and within the range reported for proven shale oil plays. The KCF shows good oil saturation in most of the modelled well locations of up to 6.4 mg/g rock, indicating potentially producible shale oil. Predictions from modelling support the interpretations from geochemical data.

1. Introduction

The exploration of unconventional resource plays (shale oil and gas) could be significant for maximising the production value in proven geological basins and facilitate the transition to cleaner energy in terms of meeting current energy security needs. According to the U.S. Energy Information Administration [1], the world's technically recoverable resource plays are estimated to amount to approximately 345 billion barrels of oil and 7299 trillion cubic feet of gas, which are significant volumes.

Overall, successful shale oil and gas reservoirs have been investigated and reported to possess a combination of ideal geochemical characteristics suitable for hydrocarbon generation, saturation, and producibility. These geochemical characteristics include total organic carbon content (TOC) equal to or greater than 2 wt%, oil-prone kerogen Type I, II or IIS, thermal maturity in the 0.6–1.4%Ro vitrinite reflectance range and oil saturation index (OSI) greater than 100 mgHC/gTOC [2–5]. The thickness of the organic-rich shale reservoir should also be equal to or greater than 15 m [5].

In the UK North Sea, the Kimmeridge Clay Formation (KCF), which was deposited during the Upper Jurassic to Lower Cretaceous rifting event, is the main source rock for oil and gas accumulations in proven conventional sandstone and carbonate reservoirs [6–8]. The source rock has the potential for shale oil and gas exploitation in the South Viking Graben area of the North Sea based on analysis of its geochemical, mineralogical, and geomechanical characteristics [9,10].

In this study, we first interpret TOC/pyrolysis and vitrinite reflectance data from KCF samples in terms of hydrocarbon generation potential (that is, kerogen quantity and type and maturity). That interpretation is combined with predictions from 1D basin modelling in terms of present day thermal maturity and residual oil saturation of the KCF at selected well locations to investigate its potential for shale oil and gas plays. This integrated approach allows for the evaluation of shale oil and gas potential in well locations where there is limited or no available geochemical data. In addition, the techniques employed here could be applied in other economically prospective areas.

The study area covers six blocks (Blocks 16–18 and 21–23) within Quadrant 15 in the Outer Moray Firth region of the UK North Sea (Fig. 1)

* Corresponding author.
E-mail address: a.akinwumiju2@unimail.derby.ac.uk (A.A. Akinwumiju).

https://doi.org/10.1016/j.uncres.2024.100098
Received 2 August 2023; Received in revised form 11 April 2024; Accepted 9 July 2024
Available online 10 July 2024

and has an area extent of approximately 1200 km^2. There are 11 conventional oil discoveries (Fig. 1) in the Upper Jurassic (Piper Formation and Claymore Member) and Lower Cretaceous (Upper Valhall Formation) sandstone reservoirs within the study area [11].

2. Geological setting

The North Sea Basin (NSB) is one of the most prolific hydrocarbon provinces in the world, with its geological evolution well-documented in several publications including the North Sea Millennium Atlas [12]; Glennie [13]; Johnson et al. [14]; Raji et al. [10], Underhill & Richardson [15] amongst others.

Evolution of the basin has been mostly attributed to Permo-Triassic and Late Jurassic-Early Cretaceous rifting events, including episodes of thermal subsidence (Fig. 2). The Permo-Triassic rifting is considered to have been initiated during the Early Permian with the production of Zechstein evaporites after active faulting ceased [16]. Thick coarse fluvial sediments were deposited during the Triassic, until a widespread north-south marine transgression marks the transition between the Triassic and Jurassic [17].

The main structural elements of the basin were developed during Late Jurassic to Early Cretaceous extension with localised, rift-associated halokinesis [14]. The KCF was deposited during this extensional phase under restricted marine conditions in water depths of about 150 to more than 200 m [11,19]. It consists of dark-grey brown to black shales, of calcareous to non-calcareous nature, interbedded with thin siltstone and sandstone layers (Fig. 2). It has a maximum depositional thickness of ~1400 m in depocenters within the Central and Northern North Sea regions [20]. Within the study area, the KCF is composed of predominantly shale lithology, and is found across the basin with reported thicknesses between 20 and 600 m [21].

3. Dataset and methodology

3.1. Geochemical characterization

The geochemical dataset used for the characterization of the Kimmeridge Clay Formation in this study was compiled from open file database of the Oil and Gas Authority, UK. These are available TOC/pyrolysis and vitrinite reflectance datasets derived from the analyses of predominantly cuttings and a few core samples from eighteen wells (Table 1). The bulk of the analysed wells are within the Witch Ground Graben, where the KCF occurs at deeper burial depths, while the remaining wells are located in the Halibut-Renee Trough and on the Claymore-Tartan Ridge and Piper Shelf, where the KCF is shallower. Geochemical interpretation graphs have been created in p:IGI + software with reference to the base true vertical depth values of samples.

3.2. 1D basin modelling

One dimensional (1D) basin models have been constructed in twenty well locations using ZetaWare's Genesis software to illustrate the burial and thermal histories in the study area. This directly impacts and allows for investigations of the maturity and hydrocarbon generation/saturation potential of the KCF.

The key inputs for modelling including lithostratigraphic/formation tops, lithologies and calibration datasets (temperature and vitrinite reflectance data) were compiled from well reports and open file database of the Oil and Gas Authority (OGA), UK. Other inputs for modelling including lithostratigraphic ages, paleo-water depth, ages of missing deposits and the timings of rifting episodes are based on information available from ICS chronostratigraphic chart ([22]; updated), completion report/composite log for wells and published literature such as White & Latin [23] and Mackay et al. [24]. Examples of stratigraphic and tectonic model inputs in Genesis in two well locations are indicated in Fig. 3.

3.2.1. Thermal boundary conditions and model calibration

In 1D modelling, the basin thermal history is normally modelled by constraining the upper and lower thermal boundary conditions. The upper boundary condition accounts for the variations in surface temperature values throughout geologic time due to changing paleo-latitudes and -water depths, while the lower boundary condition is determined by the basal heat flow [25].

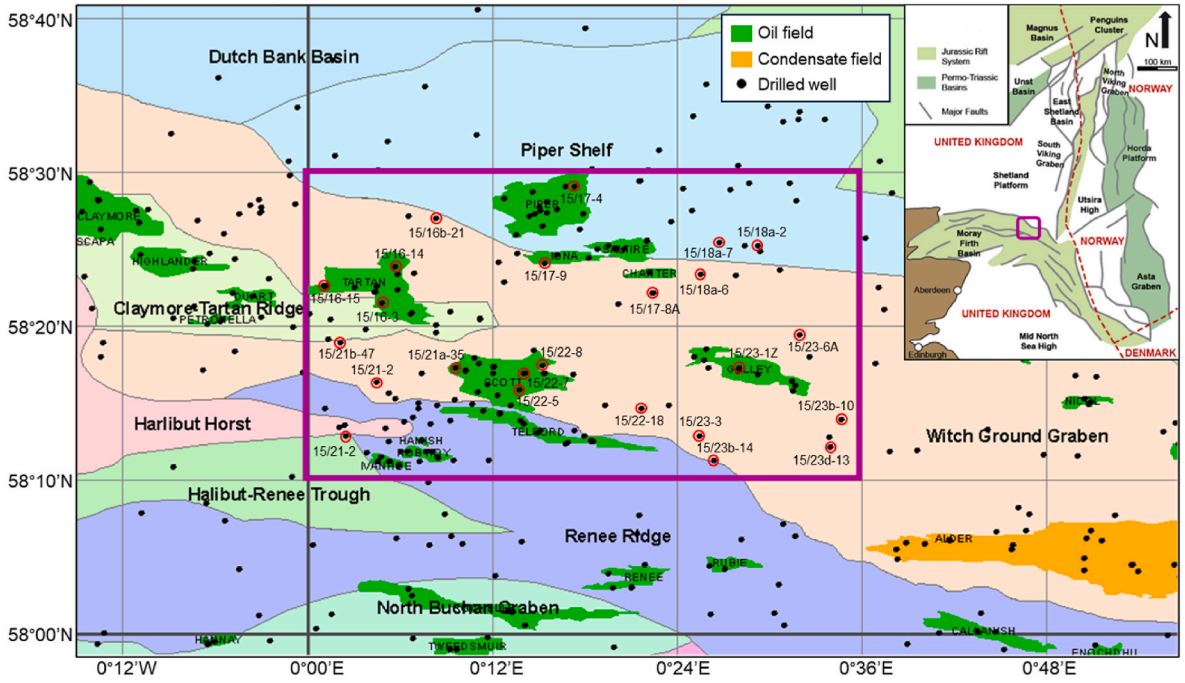

Fig. 1. Structural element map of the study area (purple box) showing existing conventional hydrocarbon accumulations. The study area encompasses Blocks 16–18 and 21–23 in Quadrant 15, Outer Moray Firth region of the UK North Sea (inset modified after [10]). The well locations used in this study are indicated in red circles.

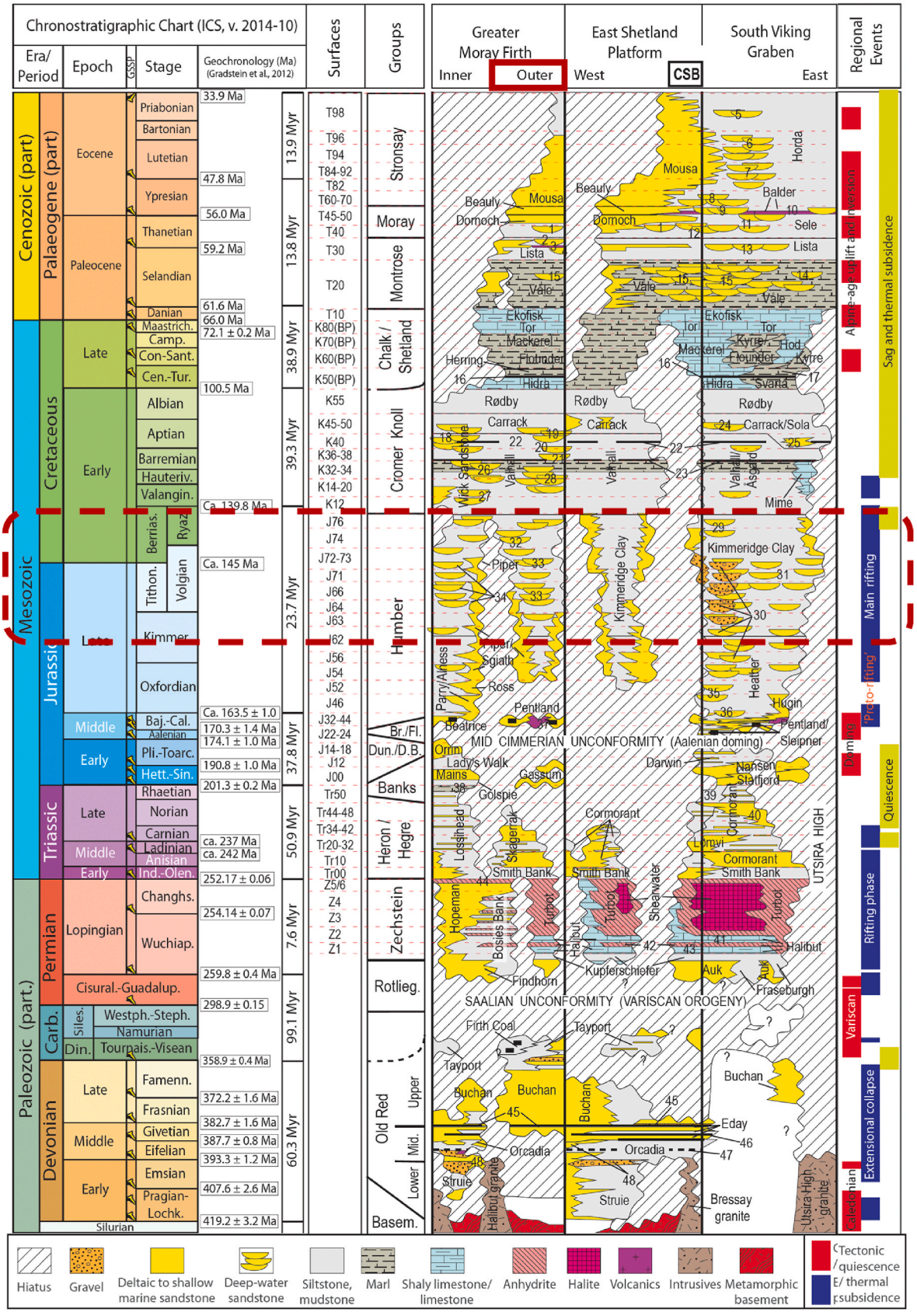

Fig. 2. Tectono-stratigraphic chart showing the regional events and KCF (dark red dashed box) in the UK North Sea (modified from [18]).

Table 1
Summary of geochemical data available for well locations in the study area.

SN	Well name	Location	Depth interval (m/MDKB)	Sample type	Number of samples		
					TOC	Pyrolysis	Vitrinite reflectance
1	15/16-1	Claymore-Tartan Ridge	2993–3020	Cuttings	6	3	n.a.
2	15/16-3	Claymore-Tartan Ridge	3068–3159	Cuttings	10	8	4
3	15/17-4	Piper Shelf	2527–2574	Cuttings	8	4	n.a.
4	15/18-2	Piper Shelf	2835–2874	Cuttings	4	1	n.a.
5	15/18a-6	Witch Ground Graben	3662–3833	Cuttings	11	11	n.a.
6	15/18a-7	Piper Shelf	3263–3267	Cuttings & sidewall core	3	3	n.a.
7	15/21-2	Witch Ground Graben	3113–3359	Cuttings	20	6	n.a.
8	15/21-5	Halibut-Renee Trough	2097–2428	Cuttings	19	13	n.a.
9	15/21b-47	Witch Ground Graben	3452–3684	Cuttings	24	24	4
10	15/22-5	Witch Ground Graben	4081–4459	sidewall core	6	6	6
11	15/22-7	Witch Ground Graben	3327–3469	Cuttings	10	10	2
12	15/22- 8	Witch Ground Graben	3600–3789	Cuttings	19	10	5
13	15/23-1Z	Witch Ground Graben	3826–3895	Cuttings	6	5	n.a.
14	15/23-2	Witch Ground Graben	3895–3900	Cuttings	1	1	n.a.
15	15/23a-12	Witch Ground Graben	3864–3882	Core	n.a.	n.a.	5
16	15/23b-10	Witch Ground Graben	4189–4216	Cuttings & core	51	20	10
17	15/23b-14	Witch Ground Graben	3917–3943	Core	n.a.	n.a.	3
18	15/23d-13	Witch Ground Graben	4379–4397	Cuttings & core	n.a.	n.a.	6

n.a., not available.

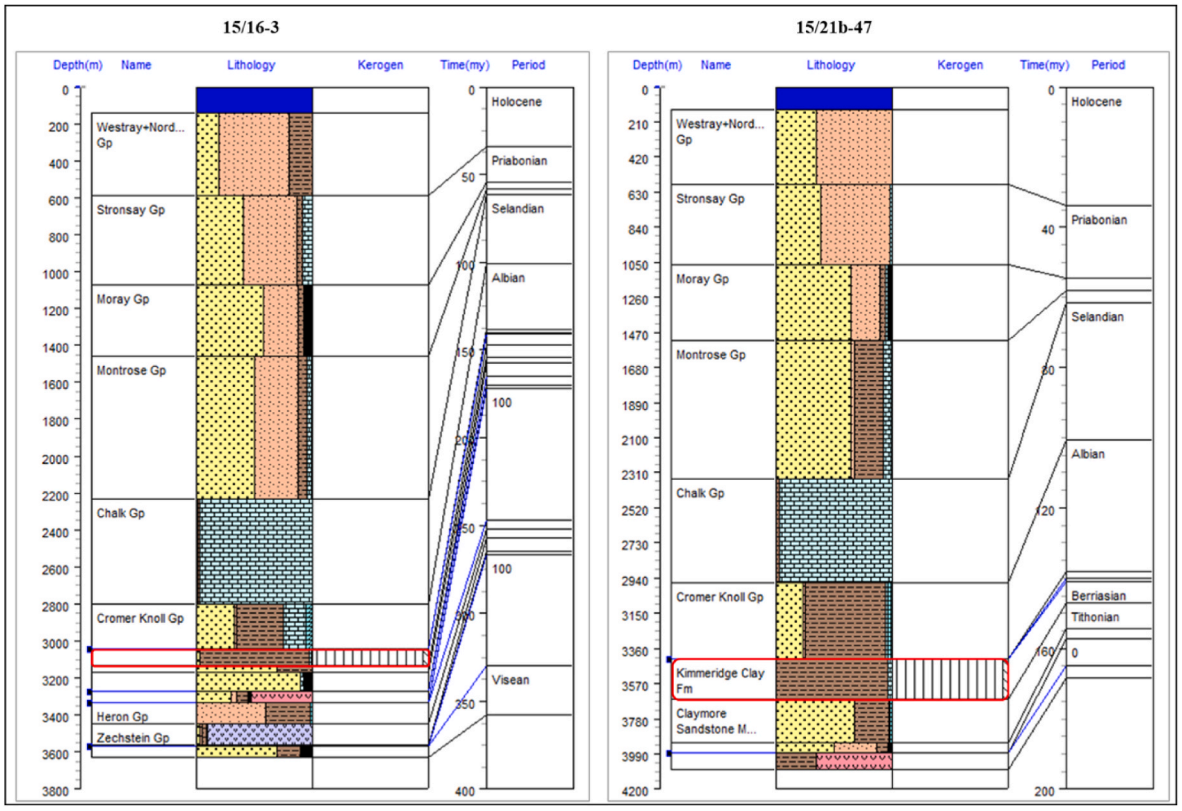

Fig. 3. Stratigraphic and tectonic model inputs in Genesis in two well locations in the study area shown in Fig. 1; KCF depth intervals in red boxes showing thickness variation.

The input paleo-sediment-water-interface temperatures for the models constructed in this study are based on published literature by Cornford [7]. For the lower thermal boundary condition, a full lithospheric model comprising thicknesses of the lithospheric mantle, lower crust and upper crust has been used with a fixed temperature of 1330 °C at the base [26].

The input lithospheric and crustal thickness (lower crust and upper crust) values of 98–100 km and 26–27 km respectively have been projected from Maystrenko and Scheck-Wenderoth [27]. These values have been constrained using gravity modelling. The 1D models were then calibrated using extracted lithospheric and crustal thicknesses for each well location to optimise the depth fit with the respective measured reservoir/Horner-corrected bottom hole temperature and vitrinite reflectance data where available (Figs. 4 and 5).

Overall, the structure of the lithosphere constrained from gravity modelling by Maystrenko and Schenk-Wenderoth [27] shows good agreement with temperature data (Fig. 4), and most of the measured vitrinite reflectance measurements from the modelled well locations in the study area (Fig. 5). We use the Easy%RoDL kinetic model, which provides the best calibration to the available vitrinite reflectance data.

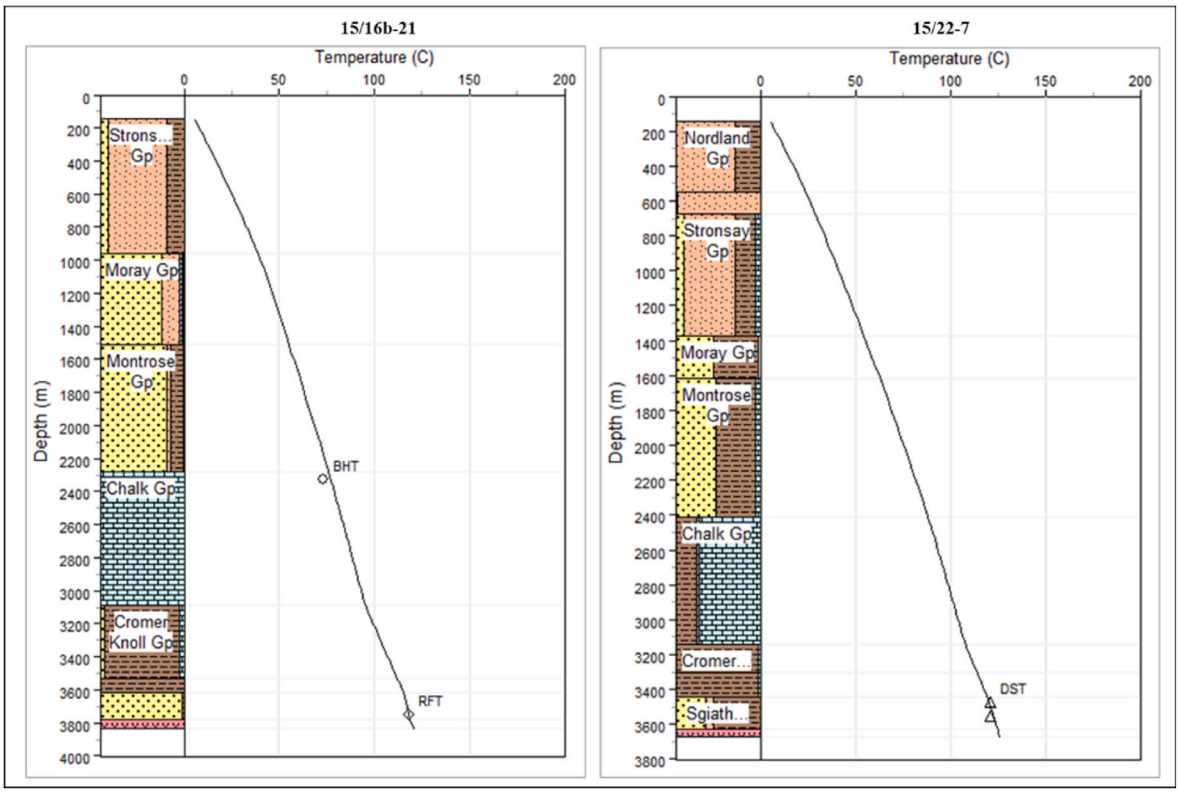

Fig. 4. Wells showing good calibration to measured reservoir/corrected bottom hole temperature values (circle, diamond & triangle symbols). Black lines represent modelled temperature with depth.

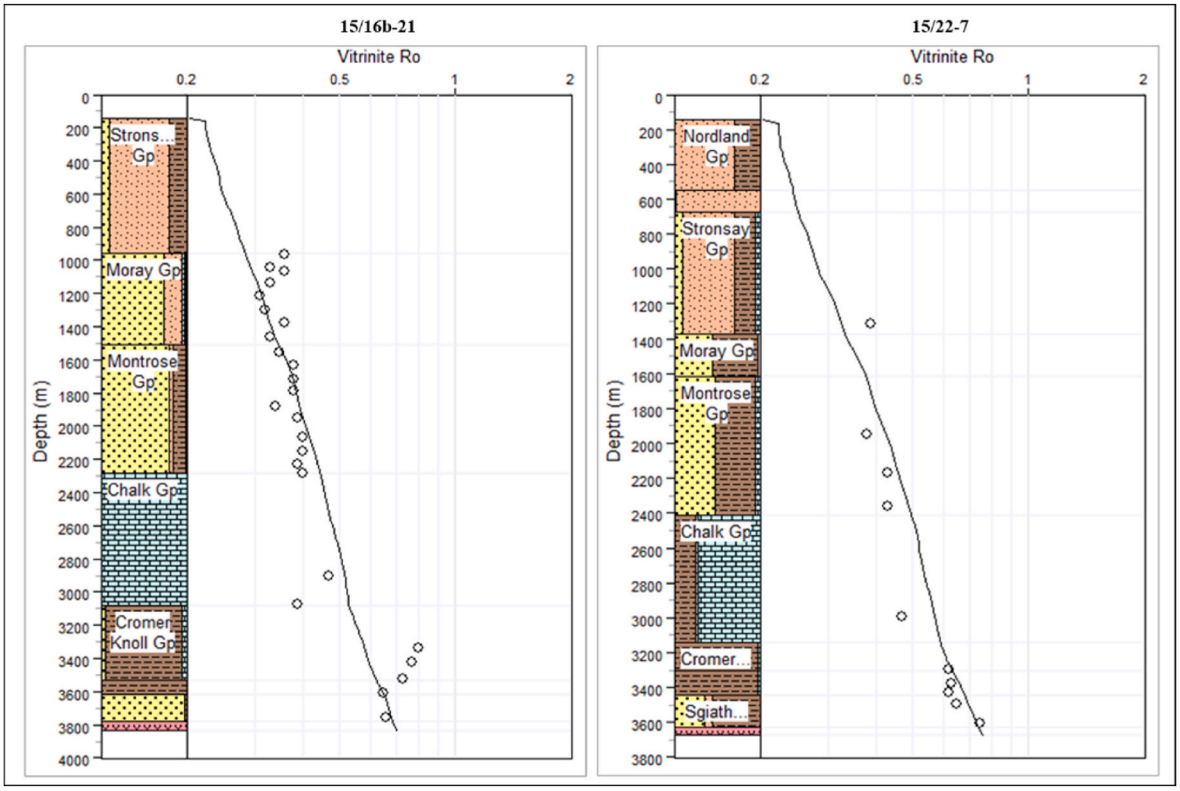

Fig. 5. Wells showing fair to good calibration to most of the measured vitrinite reflectance data points (circle symbols). Black lines represent modelled vitrinite reflectance with depth using the Easy%RoDL kinetic model [28].

3.2.2. Kimmeridge clay formation source input parameters for modelling

To model the KCF kerogen transformation and hydrocarbon generation/saturation through geologic time, original Total Organic Carbon (TOC_o) and Hydrogen Index (HI_o) were estimated from the available geochemical data using low maturity samples based on pyrolysis T_{max} values (Table 2). A mixed kerogen kinetic organofacies has been modelled for the KCF in this study using a default kerogen kinetic scheme provided in ZetaWare's Genesis software based on Pepper and Corvi [29] has shown in Table 2.

4. Results and discussion

4.1. Geochemical characterization

4.1.1. Organic richness and hydrocarbon potential

The KCF shows good to excellent organic richness in the study area with most of the samples showing TOC distribution between 2 and 10 wt % (Fig. 6). However, few samples, predominantly from wells 15/16–1, 15/18–2 & 15/21-5 show TOC values less than 2 wt%, which indicate fair to poor organic richness [7]. This may be due to sample handling or difference in methods of analysis, as the data has been acquired from the OGA data repository and we do not have control of whether all samples were analysed with the same analytical protocols.

The pyrolysis S_2 parameter is normally used to classify source rocks according to their hydrocarbon generation potential, i.e., the potential hydrocarbon yield of the kerogen upon further maturation. Typically, source rocks with initial S_2 values between 2 and 5 mg/g are considered as having only fair remaining hydrocarbon yield potential while those with initial S_2 values greater or equal to 5 mg/g are considered as having good remaining hydrocarbon yield potential [30].

A cross-plot of S_2 *versus* TOC (on a log scale) of all available samples suggests the KCF has very good hydrocarbon generation potential in the study area (Fig. 7). Higher potential is indicated in most of the samples from wells 15/17–4, 15/21–5 and 15/22–7 with TOC and S_2 values of up to 8.4 wt% and 49.4 mg/g respectively. This is probably due to very good organic matter preservation during the deposition of the KCF at these well locations.

4.1.2. Kerogen type and maturity

The type of kerogen present in a source rock is a key factor in determining the type of hydrocarbon that is likely to be generated. Interpretations from the graph of Hydrogen Index (HI) *versus* Oxygen Index (OI) (pseudo-van Krevelen diagram [31]) show that the bulk of the KCF samples in this study area plot predominantly as oil-prone Type II kerogen (Fig. 8) typically derived from bacterially degraded algae [7], while the remaining samples indicate oil/gas-prone Type II/III mixed kerogen to gas-prone Type III kerogen.

Furthermore, the graph of pyrolysis T_{max} *versus* HI (Fig. 9) suggests kerogen types that are consistent with interpretations from the pseudo-van Krevelen diagram. It is worth noting that a wide range of HI values (~100–784 mg/gTOC) shown by the KCF samples in the study area is probably due to different types of organic matter since T_{max} values suggest that the analysed samples are predominantly marginally mature (<442 °C T_{max}) for hydrocarbon generation at present day [32]. Only a few samples from wells 15/22–8 & 15/23b-10 fall within the mid-oil maturity window (442–455 °C T_{max}).

Table 2
KCF source input parameters in Genesis.

TOC_o (wt %)	HI_o (mg/gTOC)	Kerogen mix
5	400	95 % of KCF as oil-prone organofacies B-Aquatic marine clay rich 5 % of KCF as gas-prone organofacies D/E-Terrigenous terrestrial wax

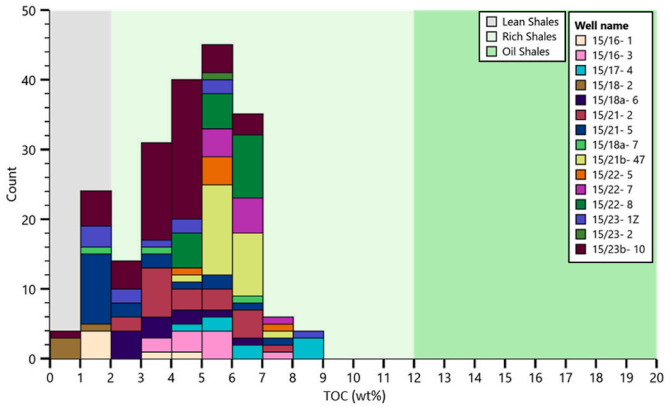

Fig. 6. TOC distribution in the KCF showing organic richness in studied wells.

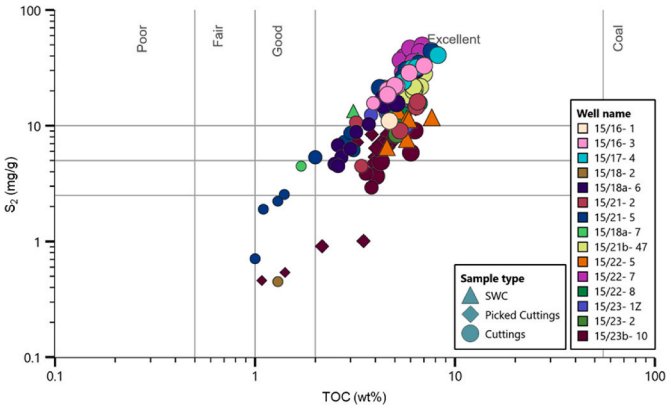

Fig. 7. Plot of S_2 *versus* TOC showing KCF hydrocarbon generation potential in wells.

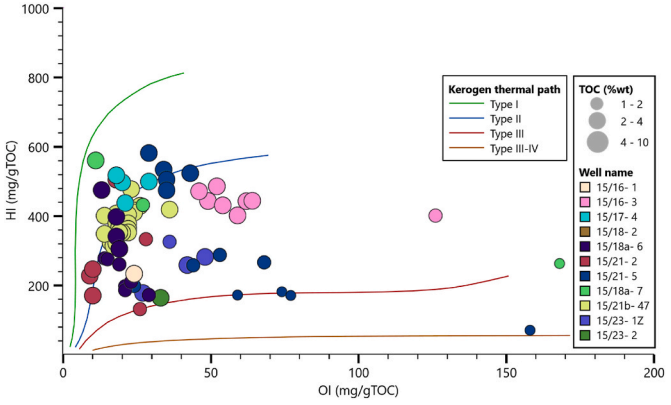

Fig. 8. Kerogen type from pseudo-van Krevelen diagram between Hydrogen Index and Oxygen Index (modified from [31]).

The available vitrinite reflectance data for the KCF interval also show that it is immature to mid-oil mature (0.41–0.91%R_o) for hydrocarbon generation at present day (Fig. 10), similar to T_{max} data. Due to the limited vitrinite reflectance data for wells in the study area, further investigation of the thermal maturity of the KCF has been conducted using 1D basin modelling, which is discussed in the subsequent paragraphs.

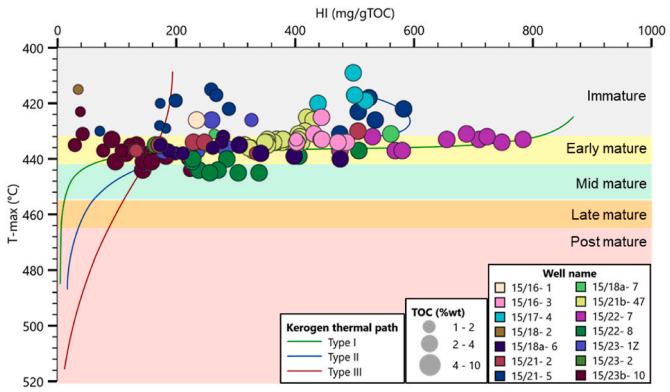

Fig. 9. Kerogen type and maturity from HI *versus* T_{max} (modified from [7,10]). Typical T_{max} maturity interpretation overlay assuming a Type II kerogen after Integrated Geochemical Interpretation Limited [33].

4.1.3. Hydrocarbon generation and saturation

Hydrocarbon generation from source rocks can be seen from increases in the pyrolysis Production Index (PI), with a PI value greater than around 0.10 indicating the onset of significant hydrocarbon generation where contamination by oil-based drilling mud and/or migrated oil is absent. Only a few studied KCF samples from wells 15/16–3, 15/18a-6, 15/21b-47 & 15/23-1Z show hydrocarbon generation using the plot of PI *versus* T_{max} (Fig. 11). The bulk of the samples from the remaining well locations show low kerogen conversion to hydrocarbon for the KCF.

For unconventional resource plays, geochemical indication of the amount of potentially producible oil is estimated by the amount of measured pyrolysis free oil (S_1) relative to TOC. This is expressed as Oil Saturation Index (OSI=S_1 mg/g/(wt% TOC/100)) which is an oil crossover effect described as when petroleum content exceeds more than 100 mgHC/g TOC pyrolysis equivalent [3]. However, it should be noted that interpretations of S_1 parameter may be impacted by the extraction of samples to remove oil-based drilling mud contaminations prior to analysis and/or evaporative losses due to sample handling, age and storage [3,4,34]. To account for evaporative losses during source rock characterization for potentially producible shale oil, a correction factor is normally applied to restore the measured S_1 values to the likely original values under reservoir conditions at depths (e.g., [3,4,35]).

A plot of the corrected S_1 values *versus* TOC indicates low oil content for majority of the studied samples (Fig. 12), with only samples from wells 15/16–3, 15/21b-47, 15/22–5 and 15/23-1Z showing good oil saturation (OSI >100 mgHC/g TOC), which is indicative of producible shale oil.

4.2. 1D basin modelling

4.2.1. Geothermal gradient and heat flow values

The results of the 1D models predict present day geothermal gradients (average) and seabed heat flow values varying from 31 °C/km to

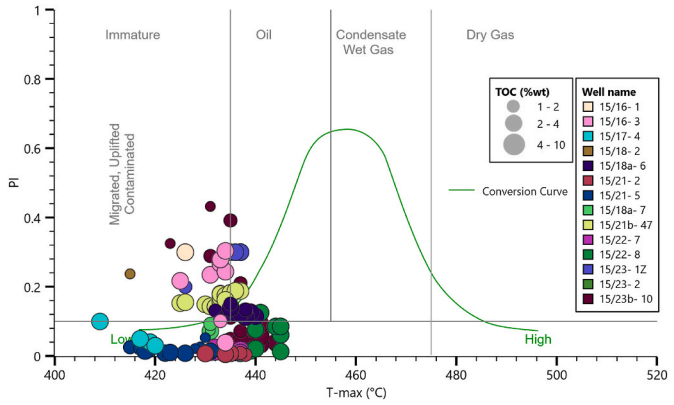

Fig. 11. Pyrolysis Production Index versus T_{max} plot showing oil generation from the KCF at some of the drilled locations in the study area.

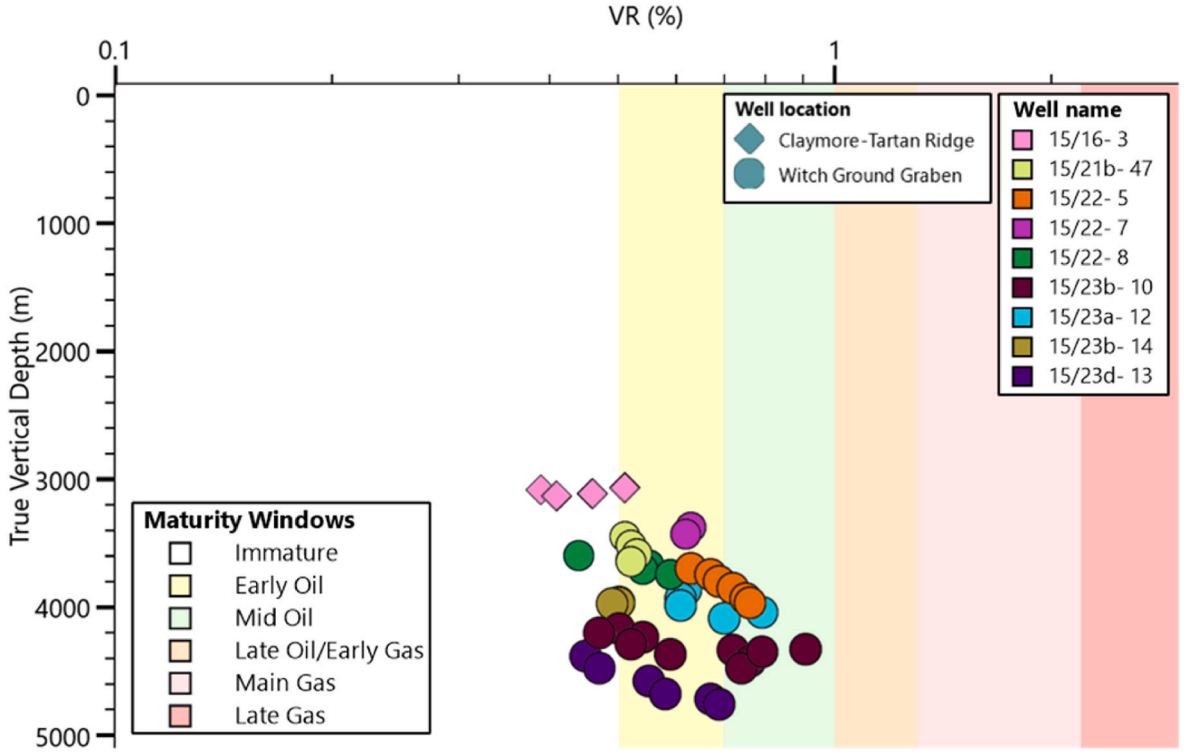

Fig. 10. Plot of available vitrinite reflectance versus depth showing the thermal maturity of the KCF in the study area.

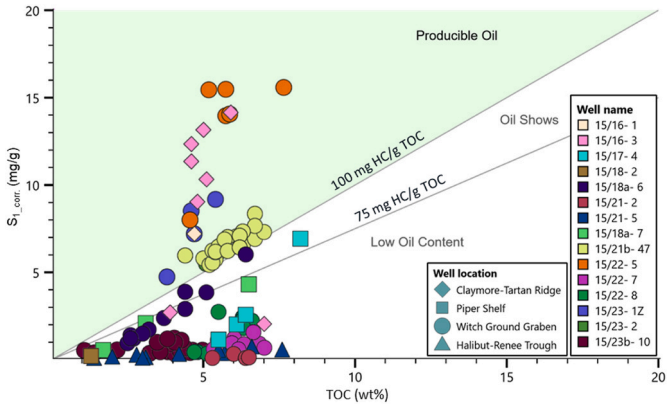

Fig. 12. Plot of the corrected S_1 values versus TOC for studied KCF samples. The correction factor applied to S_1 for evaporative loss is 1.87 [4].

37.7 °C/km and 58.1 mW/m^2 to 62.1 mW/m^2 respectively (Figs. 13–17), within the study area. The predicted heat flow values gradually increase towards the western part of the study area, while the geothermal gradients decrease along the same trend (Figs. 16 and 17). This trend probably reflects the lower thermal conductivities of the predominantly shale lithologies in the eastern part of the study area when compared to the western part. Overall, the predicted values fall within the range of published values in the study area by Kubala et al. [36].

4.2.2. KCF maturity and transformation ratio

The models predict vitrinite reflectance (VR) values between 0.51 and 1.15%R_o for the KCF. This is indicative of early-oil to late-oil/early-gas maturity window for this source rock in the study area at present day (Figs. 18 and 19). The KCF is predicted to be least mature in the western part of the study area where it buried to less than ~3.8 km depth. The modelled wells in the western part show VR values < 0.7%R_o for the KCF, which is indicative of early-oil maturity window (Fig. 19).

Also, the KCF shows higher maturities in wells 15/22–8, 15/22–18,

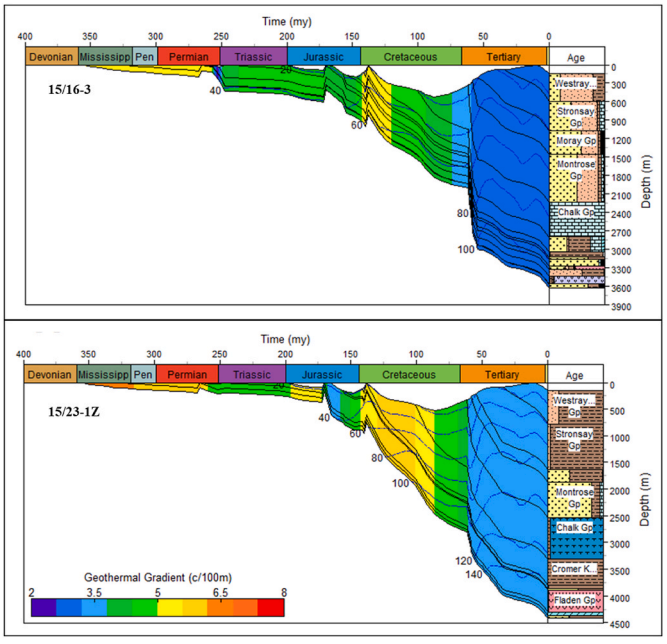

Fig. 13. Burial history profiles for wells 15/16–3 and 15/23-1Z showing geothermal gradient through geologic time with maximum burial depths for lithostratigraphic units achieved at present day. Black lines represent subsidence curves; blue lines represent isotherms (°C)).

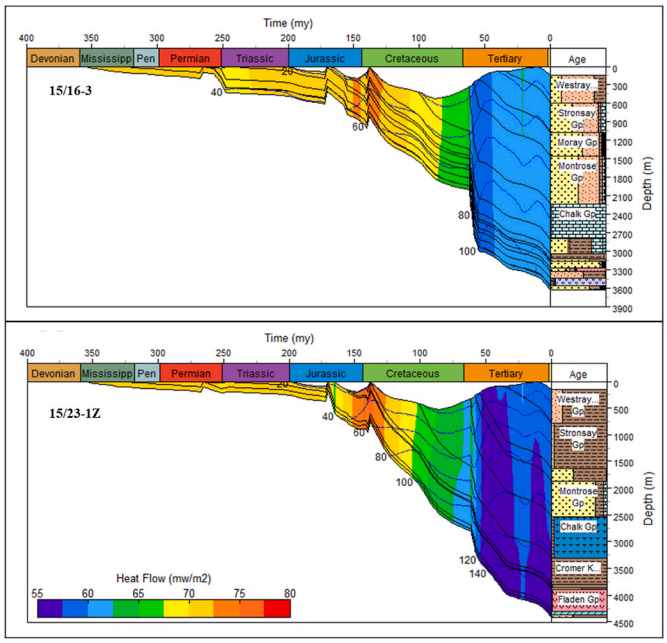

Fig. 14. Burial history profiles for wells 15/16–3 and 15/23-1Z showing heat flow through geologic time with maximum burial depths for lithostratigraphic units achieved at present day. Black lines represent subsidence curves; blue lines represent isotherms (°C)).

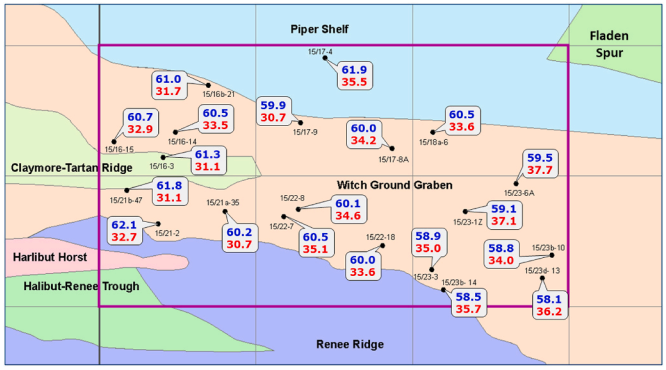

Fig. 15. Predicted present day seabed heat flow (blue) and average geothermal gradients (red) values at all modelled well locations in the study area.

15/23-1Z, 15/23–3, 15/23-6 A, 15/23b-10, 15/23b-14 & 15/23d-13 (VR values of 0.73–1.15%R_o, indicating mid-oil to late-oil/early-gas maturity window), which are situated in the eastern part of the study area (Fig. 19). This is most likely due to higher geothermal gradients (Figs. 15 and 16) and/or deeper burial depths (up to ~4.3 km) of the KCF at these well locations.

According to Hantschel and Kauerauf [37], the fraction of reactive kerogen that is converted into oil and gas is indicated by the transformation ratio (TR). Modelling results predict transformation ratios ranging between ~10 and 86 % for the KCF in the study area. The lowest TR (~10 %) is indicated in well 15/17–4 where the KCF is at the shallowest burial depth and least mature, while the highest TR (86 %) is indicated in well 15/23d-13 where the KCF is at the deepest burial depth and most mature in the study area (Figs. 19 and 20). Overall, the predicted present-day maturities and transformation ratios from 1D basin modelling show good trends with variations in the present day burial depths of KCF within the structural elements in the study area.

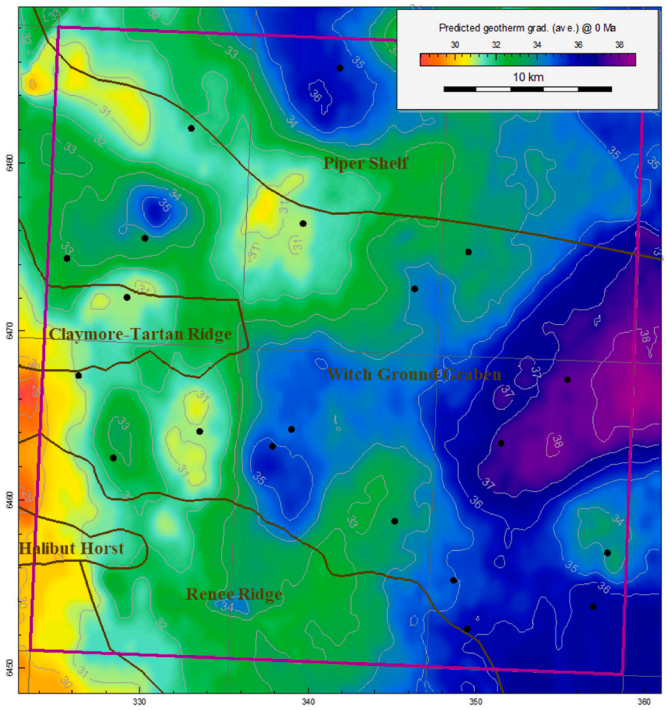

Fig. 16. Map of predicted present day average geothermal gradient. Map has been created using the correlation gridding tool in ZetaWare's Trinity software.

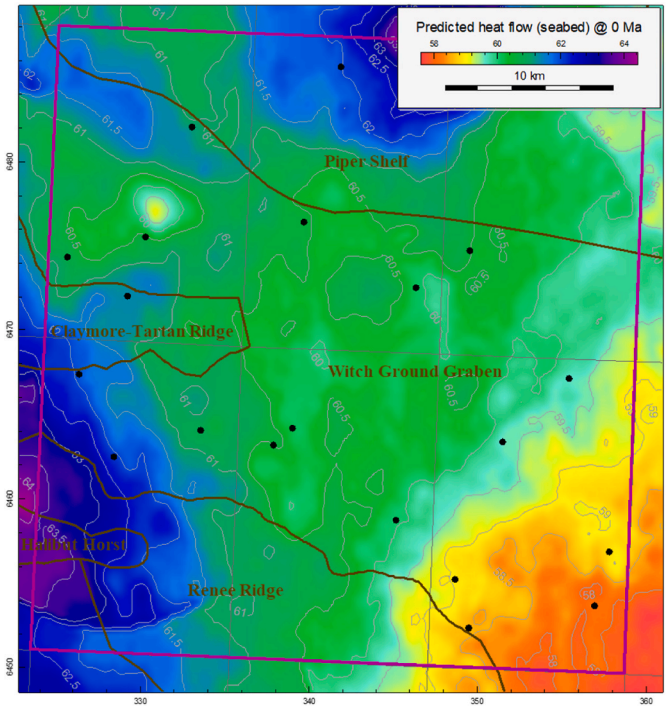

Fig. 17. Map of predicted present day seabed heat flow. Map has been created using the correlation gridding tool in ZetaWare's Trinity software.

4.2.3. *Hydrocarbon generation and saturation*

Apart from the thermal maturity, which is significant for hydrocarbon generation, organic-rich source rocks must possess good oil saturation to allow the possibility of commercial production of oil [3]. The results of 1D basin modelling indicate high oil saturation within the KCF in most of the modelled well locations at present day, with predicted values mostly greater than 5 mg/g rock (Figs. 21 and 22). The predicted

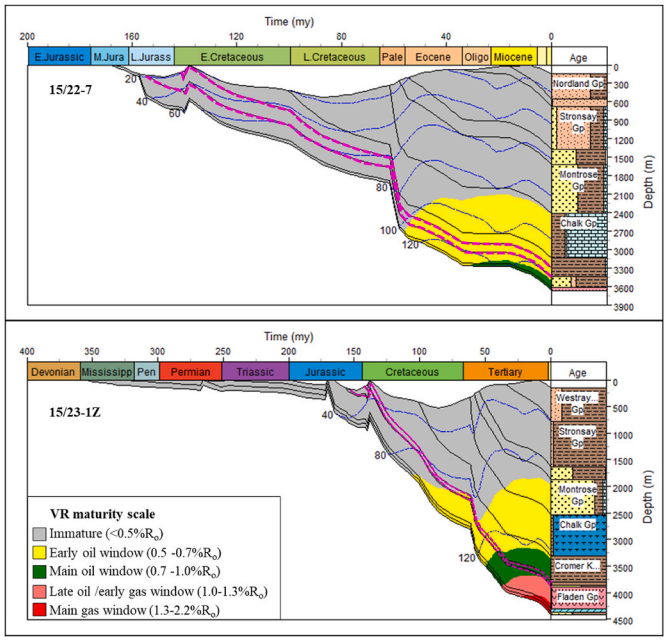

Fig. 18. Burial history profiles for wells 15/22–7 and 15/23-1Z showing modelled Easy%RoDL maturity through geologic time. KCF interval is indicated in dashed purple lines. Black lines represent subsidence curves; blue lines represent isotherms (°C)).

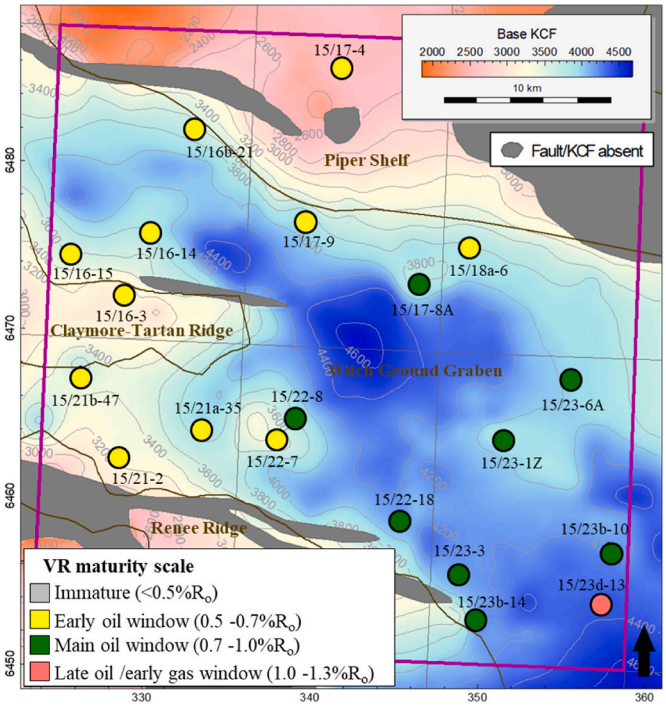

Fig. 19. Modelled present day KCF vitrinite reflectance thermal maturity for hydrocarbon generation at well locations.

values gradually increase towards the western part of the study area within the Witch Ground Graben, with higher values of about 6.3 and 6.4 mg/g rock indicated in wells 15/21–2 and 15/22–7 respectively. This trend is reflective of increasing KCF maturities from early-oil window to late-oil/early gas window towards the eastern part of the study area within the Witch Ground Graben (Fig. 19).

We noticed that the results of 1D basin modelling have predicted

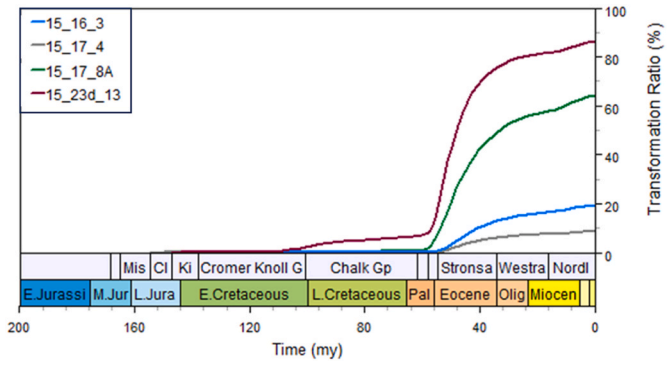

Fig. 20. Modelled KCF kerogen transformation through geologic time at some of the well locations in the study area.

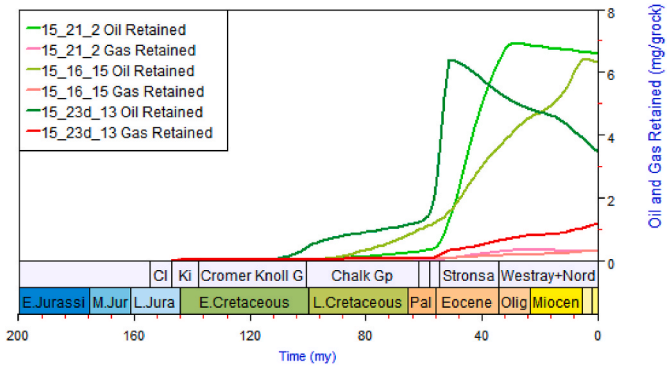

Fig. 21. Modelled KCF hydrocarbon saturation through geologic time at some of the well locations in the study area.

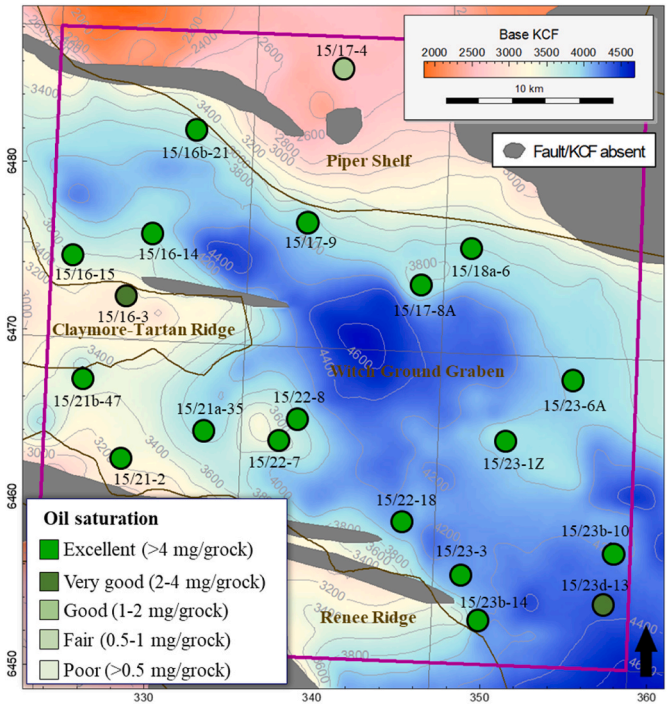

Fig. 22. Modelled KCF oil saturation at present day in all studied wells in the project area. The modelled wells except 15/17–4 exhibit very good to excellent oil saturation.

good oil saturation within the KCF at more drilled locations in the study area when compared to interpretations from available geochemical data (Fig. 12). We consider the predicted oil saturation from 1D basin modelling to be more representative of the KCF in the study area. However, only minor quantities of gas have been predicted to be retained in the KCF at modelled well locations, which is not unexpected since the KCF has been indicated to lie mainly within the oil-generation window at present day in the study area (Fig. 19).

5. Conclusions

The interpretation of total organic carbon/pyrolysis and vitrinite reflectance data from eighteen drilled locations has been combined with 1D basin modelling of twenty well locations to investigate the potential of shale oil and gas exploitation from the Kimmeridge Clay Formation in the Outer Moray Firth region of the UK North Sea. Interpretations from the geochemical data has suggested that the Kimmeridge Clay Formation has a very good hydrocarbon generation potential in the study area with mean TOC and pyrolysis S_2 values of approximately 5 wt% and 20.7 mg/g respectively. These shales contain predominantly oil-prone Type II kerogen, while few samples indicate mixed oil/gas-prone Type II/III to gas-prone Type III kerogen.

Furthermore, the available geochemical data suggests that the Kimmeridge Clay Formation lies predominantly within early-to main-oil window maturity at present day. Higher maturities (main-oil window) are shown by samples from the wells within the Witch Ground Graben in the eastern section of the study area where the Kimmeridge Clay Formation occurs at deeper burial depths of up to 4.3 km. In general, most of the samples evaluated from wells 15/16–3, 15/21b-47, 15/22–7, 15/23–2 & 15/23-1Z show significant oil saturation index above 100 mgHC/gTOC, which is indicative of a good potential for producible shale oil.

The results of 1D basin modelling predict present day average geothermal gradients and seabed heat flow values varying from 31 °C/km to 37.7 °C/km and 58.1 mW/m^2 to 62.1 mW/m^2 respectively. The predicted heat flow values gradually increase towards the western part of the study area, while the geothermal gradients decrease along the same trend. This is reflective of the lower thermal conductivities of the predominantly shale lithologies and slightly thinner crust in the eastern part of the study area.

The results of 1D basin modelling have also indicated that the Kimmeridge Clay Formation lies within early oil to late oil/early gas generation maturity window at present day in the study area, with transformation ratio values ranging between ~10 and 86 %. These predicted present-day maturities and transformation ratios show good trends with variations in the present day burial depths of the Kimmeridge Clay Formation within the structural elements in the study area.

Most of the modelled well locations show very good potential for residual shale oil. This residual shale oil may be significant in volume, particularly within the Witch Ground Graben in the western part of the study area where the Kimmeridge Clay Formation lies mainly within the early-oil window maturity at present day and higher oil saturation values have been indicated. The predicted oil saturation values are generally lower in the eastern part of the study area where the Kimmeridge Clay Formation occurs at deeper burial depths (up to about 4.3 km) and a higher maturity (main-oil to late-oil/early-gas window), most likely as a result of expulsion of the bulk of the generated oil. However, the lowest oil saturation has been indicated on the Piper Shelf where the KCF occurs at a shallower burial depth of less than 3.4 km. Overall, the results of 1D basin modelling have indicated very good oil saturation within the KCF in more wells than suggested by interpretations from available pyrolysis data in the study area.

This study has documented the usefulness of 1D basin modelling in the investigation of hydrocarbon saturation for potential resource plays in proven geological basins when combined with geochemical data. It is especially very useful for determination of present day thermal

maturities and hydrocarbon saturations in source rocks where available pyrolysis data is not from the analysis of cores samples, which are most ideal for geochemical analysis, and pyrolysis S_1 data may have been impacted by the extraction of samples to remove oil-based drilling mud contaminations prior to analysis. Another source of potential error regarding pyrolysis S_1 is evaporative loss due to sample handling, age and storage.

CRediT authorship contribution statement

Akinniyi A. Akinwumiju: Conceptualization, Data curation, Formal analysis, Investigation, Validation, Visualization, Writing – original draft, Writing – review & editing. **Dorothy Satterfield:** Supervision, Writing – review & editing, Conceptualization.

Declaration of competing interest

The authors declare that they have no known competing financial interests or personal relationships that could have appeared to influence the work reported in this paper.

Acknowledgments

The authors would like to thank the Oil and Gas Authority, UK for making the database used in this study publicly available. A special thanks goes to Integrated Geochemical Interpretation Limited (IGI Ltd.) for the use of their p: IGI + software for geochemical data visualisation and interpretation and ZetaWare Incorporated for their generous donation of Genesis and Trinity software student licenses for this study. Jim Armstrong is greatly acknowledged for his constructive feedback on this work.

Appendix A. Supplementary data

Supplementary data to this article can be found online at https://doi.org/10.1016/j.uncres.2024.100098.

References

[1] U.S. Energy Information Administration, Technically Recoverable shale oil and shale gas resources: an assessment of 137 shale formations in 41 countries outside the United States [online], Available at: https://www.actu-environnement.com/media/pdf/news-23433-rapport-aie.pdf, 2013.
[2] D.M. Jarvie, Shale resource systems for oil and gas: Part 1—shale-gas resource systems, in: J.A. Breyer (Ed.), Shale Reservoirs—Giant Resources for the 21st Century, 97, AAPG Memoir, 2012, pp. 69–87.
[3] D.M. Jarvie, Shale resource systems for oil and gas: Part 2— shale-oil resource systems, in: J.A. Breyer (Ed.), Shale Reservoirs—Giant Resources for the 21st Century, 97, AAPG Memoir, 2012, pp. 89–119.
[4] I.J. Andrews, The Jurassic Shales of the Weald Basin: Geology and Shale Oil and Shale Gas Resource Estimation, British Geological Survey for Department of Energy and Climate Change, London, UK, 2014.
[5] Z. Jiang, W. Zhang, C. Liang, Y. Wang, H. Liu, X. Chen, Basic characteristics and evaluation of shale oil reservoirs, Petroleum Research 1 (2016) 49–163, https://doi.org/10.1016/S2096-2495(17)30039-X.
[6] B.S. Cooper, P.C. Barnard, N. Telnaes, The Kimmeridge Clay Formation of the North Sea, in: B.J. Katz (Ed.), Petroleum Source Rocks, Springer-Verlag, Berlin, 1995, pp. 89–110.
[7] C. Cornford, Source rocks and hydrocarbons of the North Sea, in: K.W. Glennie (Ed.), Petroleum Geology of the North Sea, fourth ed.s, Blackwell Science Ltd., London, 1998, pp. 376–462.
[8] D.L. Gautier, Kimmeridgian Shales Total Petroleum System of the North Sea Graben Province, 2204-C, U.S. Geological Survey Bulletin, 2005, p. 24. http://pubs.usgs.gov/bul/2204/c.
[9] C. Cornford, B. Birdsong, M. Groves-Gidney, Offshore unconventional oil from the Kimmeridge Clay Formation of the North Sea: a technical and economic case, in: Unconventional Resources Technology Conference Proceedings, 2014. August 25-27, 2014.
[10] M. Raji, D.R. Gröcke, H.C. Greenwell, J.G. Gluyas, C. Cornford, The effect of interbedding on shale reservoir properties, Mar. Petrol. Geol. 67 (2015) 154–169.
[11] S.I. Fraser, A.M. Robinson, H.D. Johnson, J.R. Underhill, D.G.A. Kadolsky, R. Connell, P. Johannessen, R. Ravnås, Upper jurassic, in: D. Evans, C. Graham, A. Armour, P. Bathurst (Eds.), The Millennium Atlas: Petroleum Geology of the Central and Northern North Sea, Geological Society, London, 2002, pp. 157–189, 2003.
[12] D. Evans, C. Graham, A. Armour, P. Bathurst, The Millennium Atlas: Petroleum Geology of the Central and Northern North Sea, 2003. Geological Society, London, 17-33.
[13] K.W. Glennie, Petroleum geology of the North Sea; basic concepts and recent advances, Blackwell Science Geology and Petroleum Geology (1998) 636–658. Oxford.
[14] H. Johnson, A.B. Leslie, C.K. Wilson, I.J. Andrews, R.M. Cooper, Middle jurassic, upper jurassic and lower cretaceous of the UK central and Northern North Sea, 42, British Geological Survey Research Report, RR/03/001 (2005).
[15] J.R. Underhill, N. Richardson, Geological controls on petroleum plays and future opportunities in the North Sea rift super basin, AAPG (Am. Assoc. Pet. Geol.) Bull. 106 (3) (2022) 573–631, https://doi.org/10.1306/07132120084.
[16] N.A. Hodgson, J. Farnsworth, A.J. Fraser, Salt-related tectonics, sedimentation and hydrocarbon plays in the central graben, North Sea UKCS, in: R.F.P. Hardman (Ed.), Exploration Britain: Geological Insights for the Next Decade, 67, Geological Society, London, Special Publications, 1992, pp. 31–63.
[17] M.P. Coward, J.F. Dewey, M. Hempton, J. Holroyd, M.A. Mange, Tectonic evolution, in: D. Evans, C. Graham, A. Armour, P. Bathurst (Eds.), The Millennium Atlas: Petroleum Geology of the Central and Northern North Sea, Geological Society, London, 2003, pp. 17–33, 2003.
[18] S. Patruno, W. Reid, New plays on the greater east shetland platform (UKCS quadrants 3, 8-9, 14-16) – part 1: regional setting and a working petroleum system, First Break 34 (2016) 33–45, https://doi.org/10.3997/1365-2397.2016016.
[19] R. Gallois, The Kimmeridge Clay: the most intensively studied formation in Britain, Journal Open University Geological Society 25 (2) (2004) 33–38.
[20] British Geological Survey, Kimmeridge Clay Formation [Online]. Available at: https://webapps.bgs.ac.uk/lexicon/lexicon.cfm?pub=KC, 2022.
[21] Oil and Gas Authority, UK, UKCS Petroleum Systems Project: Year 1, 2019. https://data-ogauthority.opendata.arcgis.com/documents/2da8146dc00044cbbfee9e1309602d1c/about.
[22] K.M. Cohen, S.C. Finney, P.L. Gibbard, J.-X. Fan, Updated. The ICS international chronostratigraphic chart, Episodes 36 (2013) 199–204.
[23] N. White, D. Latin, Subsidence analyses from the North Sea 'triple-junction', J. Geol. Soc. 150 (1993) 473–488.
[24] L.M. Mackay, J. Turner, S.M. Jones, N.J. White, Cenozoic vertical motions in the Moray Firth basin associated with initiation of the Iceland plume, Tectonics 24 (2005) TC5004, https://doi.org/10.1029/2004TC001683.
[25] Y. Tong, D.E. Ibarra, J.K. Caves, T. Mukerji, S.A. Graham, Constraining basin thermal history and petroleum generation using palaeoclimate data in the Piceance Basin, Colorado, Basin Res. 29 (2017) 542–553, https://doi.org/10.1111/bre.12213.
[26] ZetaWare, Introduction to Thermal History, 2012. http://www.zetaware.com/support/genesis/intro/intro4.html.
[27] Y.P. Maystrenko, M. Schenk-Wenderoth, 3D lithosphere-scale density model of Central European Basin System and adjacent areas, Tectonophysics 601 (2013) 53–77.
[28] A. Burnham, Evolution of Vitrinite Reflectance Models, Presentation to Linked-In Petroleum Systems Analysts, 2016. https://www.youtube.com/watch?v=rOYNujm80uU.
[29] A.S. Pepper, P.J. Corvi, Simple kinetic models of petroleum formation. Part I: oil and gas generation from kerogen, Mar. Petrol. Geol. 12 (3) (1995) 291–319.
[30] B.P. Tissot, D.H. Welte, Diagenesis, catagenesis and metagenesis of organic matter. Petroleum Formation and Occurrence, Springer-Verlag, New York, 1984.
[31] P.C. Hackley, C.C. Walters, R.M. Kelemen, M. Mastalerz, H.A. Lowers, Organic petrology and micro-spectroscopy of Tasmanites microfossils: applications to kerogen transformations in the early oil window, Org. Geochem. 114 (2017) 23–44.
[32] J. Espitalie, G. Deroo, F. Marquis, Rock Eval pyrolysis and its applications, Rev. Inst. Fr. Petrol 40 (1985) 563.
[33] Integrated Geochemical Interpretation Limited, Rock-eval interpretation for source rocks. https://ignet.igiltd.com/main-manual/interpretation-of-geochemical-data/interpretation-by-technique/rock-eval-pyrolysis/rock-eval-interpretation-for-source-rocks/, 2019.
[34] C. Jiang, A. Mort, H. Sanei, Z. Chen, M. Milovic, R. Robinson, S_1 peak of Rock-Eval analysis: what does it represent for unconventional hydrocarbon resource assessment? GeoConvention: Geoscience New Horizons (2015). Calgary, AB Canada, May 2015, www.researchgate.net/publication/280255390.
[35] G.E. Michael, J. Packwood, A. Holba, Determination of in-situ hydrocarbon volumes in liquid rich shale plays. Unconventional Resources Technology Conference, 2013. Denver, Colorado, USA, August 2013, www.searchanddiscovery.com/pdfz/documents/2014/80365michael/ndx_michael.pdf.html.
[36] M. Kubala, M. Bastow, S. Thompson, I. Scotchman, K. Oygard, Geothermal regime, petroleum generation and migration, in: D. Evans, C. Graham, A. Armour, P. Bathurst (Eds.), The Millennium Atlas: Petroleum Geology of the Central and Northern North Sea, Geological Society, London, 2003, pp. 289–315, 2003.
[37] T. Hantschel, A.I. Kauerauf, Fundamentals of Basin and Petroleum Systems Modeling, 485, Springer Science & Business Media, 2009.